Structure−Property Relationship of Permutite-like Amorphous Silicates, $Na_{x+2y}M^{3+}{}_xSi_{1-x}O_{2+y}$ (M^{3+} = Al, Mn, Fe, Y), for Ion-Exchange Reactions

Jason D. Pless,† Robert S. Maxwell,‡ Mark L. F. Philips,† Katheryn B. Helean,† Marlene Y. Axness,† and Tina M. Nenoff*,†

Sandia National Laboratories, Post Office Box 5800, MS 0734, Albuquerque, New Mexico 87185-0734, and Lawrence Livermore National Laboratory, 7000 East Avenue, L-231, Livermore, California 94550

Received March 10, 2005. Revised Manuscript Received July 20, 2005

A series of amorphous silicate materials with the general formula $Na_{x+2y}M^{3+}{}_xSi_{1-x}O_{2+y}$ (M^{3+} = Al, Mn, Fe, Y) were studied. Samples were synthesized by a precipitation reaction at room temperature. The results indicate that the ion-exchange capacity (IEC) decreases as follows: Al > Fe > Mn > Y. Additionally, the IEC increases with increasing aluminum concentration. Structural studies show that the relative amount of octahedrally coordinated aluminum increases with increasing Al content, as does the total amount of AlO_4 species increases. The data suggest that the IEC value of these amorphous aluminosilicates is dependent on the tetrahedrally coordinated aluminum. Regeneration of the Al-silicate with acetic acid does not decrease the IEC significantly.

Introduction

Fresh water is necessary for life, and nearly one-quarter of the world's population lack an adequate fresh water supply.[1] Therefore, desalination of brackish water is important for arid and costal areas. The optimization of desalination processes requires the development of operations based on low-cost materials with high salt-removal efficiencies. Ion exchange is a promising technique among other potential methods, such as reverse osmosis, electro-dialysis, oxidation, and ultra-filtration. In utilizing this approach, the ion-exchange materials need to be robust, cheap and easy to regenerate and not result in secondary water pollution. Aluminosilicates meet many of these materials requirements.

The first aluminosilicate ion exchangers were synthesized in 1903.[2] Since then the ion-exchange and structural properties of several natural aluminosilicates, such as bentonite, chabazite, clinoptile, illite, and mordenite, have been extensively studied.[3−7] The ion-exchange ability of the first amorphous aluminosilicate used to commercially soften water, permutite,[8] has been widely studied.[9−17] The ideal composition of permutite has been reported as $Na_2Al_2Si_2O_8 \cdot H_2O$.[18]

Initial studies of permutite showed that sodium ions replace magnesium, potassium, calcium, iron, and manganese in molar proportions.[13] Further studies indicated that the ion-exchange reaction between alkaline earth metals and permutite was reversible[14] and that calcium could displace magnesium bound to permutite.[14,15] Kinetic studies indicated that the exchange of alkali metals and ammonium by protons is independent of solution concentration.[16] Similar results were reported for the exchange of divalent ions (magnesium, calcium, strontium, and barium) with copper.[17] However, dilution was found to influence aliovalent ion exchange, and the ion-exchange equilibrium increased with increasing atomic weight of the metal ion.[17]

In the present work, a systematic study of a permutite-like family of amorphous silicates ($Na_{x+2y}M^{3+}{}_xSi_{1-x}O_{2+y}$; M^{3+} = Al, Mn, Fe, Y), named generally as permutite, has been undertaken to better define the structure/property relationship in these materials and understand the ion-exchange process. The study includes a detailed synthesis, structural characterization, and ionic exchange capacity (IEC) measurements and the results are related to the local structure to the ion-exchange properties.

Experimental Section

Synthesis. Thirteen samples of permutite were prepared (Table 1) by a precipitation reaction at room temperature. A M^{3+} nitrate salt ($Al(NO_3)_3 \cdot 9H_2O$, 98%, Alfa Aesar; $Mn(NO_3)_3$, 50% solution,

* Corresponding author. E-mail: tmnenof@sandia.gov. Tel.: (505) 844 0340.
† Sandia National Laboratories.
‡ Lawrence Livermore National Laboratory.

(1) Fiorenza, G.; Sharma, V. K.; Braccio, G. *Energy Conserv. Manage.* **2003**, *44*, 2217.
(2) Harms, F.; Rumpler, A. 5th *Int. Congr. Pure Appl. Chem.* **1903**, *50*.
(3) Tymochowicz, S. *Nukleonika* **1978**, *23*, 237.
(4) Duffy, S. C.; Rees, L. V. C. *J. Chem. Soc., Faraday Trans. 1* **1974**, *70*, 777.
(5) Howery, D. G.; Thomas, H. C. *J. Phys. Chem.* **1965**, *69*, 531.
(6) Beckett, P. H. T.; Nafady, M. H. M. *Soil Sci.* **1967**, *103*, 410.
(7) Rao, A.; Rees, L. V. C. *Trans. Faraday Soc.* **1966**, *62*, 2505.
(8) Gans, R. *Jahrb. Preuss Geol. Landesanstalt (Berlin)* **1905**, *26*, 179.
(9) Günther−Schulze, V. *Z. Phys. Chem.* **1914**, *89*, 168.
(10) Kornfeld, G. *Z. Elektrochem.* **1917**, *23*, 173.
(11) Günther−Schulze, V. *Z. Elektrochem.* **1917**, *28*, 85.
(12) Levi, V. H. W.; Miekeley, N. *Radiochim. Acta* **1972**, *18*, 138.
(13) Kolb, A. *Chem.-Zeit.* **1911**, *35*, 1393.
(14) Bahrdt, A. *Chem. Ind.* **1914**, *37*, 122.
(15) Mezger, R. *J. Gasebeleucht.* **1920**, *63*, 644.
(16) Ramann, E.; März, S.; Biesenberger, K.; Spengel, A. *Z. Anorg. Chem.* **1916**, *95*, 115.
(17) Rothmund, V.; Kornfeld, G. *Z. Anorg. Chem.* **1919**, *108*, 215.
(18) Gans, R. *Chem. Ind.* **1909**, *32*, 197.

10.1021/cm050547i CCC: $30.25
Published on Web 08/30/2005

Table 1. Physical Properties of Permutite Samples

ref. label	SiO_2/ Na_2O weight ratio	targeted formulation	Si/Al mole ratio by EDS[a]	BET surface area[a] ($m^2\ g^{-1}$)	pore diameter[a] (nm)	IEC (mequiv g^{-1})	physical appearance
A1	2.40	Na_ySiO_{2+y}	1.00/0.00 (1.00/0.00)	515.5 (454.1)	3.6 (3.8)	0.86	white
A2	2.40	$Na_{0.1+2y}Al_{0.05}Si_{0.95}O_{2+y}$	0.948/0.052 (0.946/ 0.054)	361.4 (396.6)	5.8 (5.7)	0.97	white
A3	2.40	$Na_{0.2+2y}Al_{0.10}Si_{0.90}O_{2+y}$	0.897/0.103 (0.899/ 0.101)	349.1 (466.6)	5.3 (4.6)	1.68	white
A4/ C1	2.40	$Na_{0.3+2y}Al_{0.15}Si_{0.85}O_{2+y}$	0.848/0.152 (0.851/ 0.149)	457.3 (478.5)	3.0 (3.2)	1.88	white
A5	2.40	$Na_{0.4+2y}Al_{0.20}Si_{0.80}O_{2+y}$	0.799/0.201 (0.811/ 0.189)	431.1 (462.0)	(3.6) (3.7)	2.16	white
A6/ B3	2.40	$Na_{0.456+2y}Al_{0.228}Si_{0.772}O_{2+y}$	0.777/0.223 (0.769/ 0.231)	390.8 (387.6)	6.6 (7.1)	2.32	white
A7	2.40	$Na_{0.5+2y}Al_{0.25}Si_{0.75}O_{2+y}$	0.750/0.240 (0.754/ 0.246)	433.6 (434.4)	3.5 (3.1)	2.04	white
B1	1.60	$Na_{0.456+2y}Al_{0.228}Si_{0.772}O_{2+y}$	0.776/0.224 (0.778/ 0.221)	160.7 (136.2)	11.0 (9.3)	2.45	white
B2	2.00	$Na_{0.456+2y}Al_{0.228}Si_{0.772}O_{2+y}$	0.776/0.224 (0.787/ 0.213)	170.8 (257.2)	10.4 (8.0)	2.34	white
B4	3.22	$Na_{0.456+2y}Al_{0.228}Si_{0.772}O_{2+y}$	0.779/0.221 (0.783/ 0.217)	463.0 (459.0)	5.3 (5.1)	1.92	white
C2	2.40	$Na_{0.3+2y}Mn_{0.15}Si_{0.85}O_{2+y}$	N/A	235.9 (528.3)	5.2 (6.0)	1.11	brown
C3	2.40	$Na_{0.3+2y}Fe_{0.15}Si_{0.85}O_{2+y}$	N/A	390.3 (473.0)	5.1 (5.2)	1.29	orange
C4	2.40	$Na_{0.3+2y}Y_{0.15}Si_{0.85}O_{2+y}$	N/A	271.8 (560.8)	7.7 (6.9)	1.10	white

[a] The values in parentheses are for the acid-treated samples.

Alfa Aesar; $Fe(NO_3)_3{\cdot}9H_2O$, Fisher; or $Y(NO_3)_3{\cdot}6H_2O$, 99.9%, Alfa Aesar) was dissolved in distilled water at room temperature, to a concentration of approximately 3 M. In a separate beaker, a stoichiometric amount of sodium silicate solution (PQ Corporation, Solutions B-W 50, 1.60 SiO_2/Na_2O wt ratio; C, 2.00 SiO_2/Na_2O wt ratio; RU, 2.40 SiO_2/Na_2O wt ratio; or STIXSO RR, 3.20 SiO_2/Na_2O wt ratio) was added to 100 mL of distilled water. Both solutions were stirred at room temperature for 30 min. Permutite was precipitated by the slow addition of the metal nitrate solution to the silicate solution with stirring. The pH of the final solution was adjusted with HNO_3 (Fisher) to between 3 and 4 for the Al samples and to approximately 7 for samples containing Mn, Fe, and Y to ensure complete precipitation. For comparison, a sample of amorphous silica was prepared by adjusting the pH of a sodium silicate solution to ~3 with HNO_3. The products were filtered and repeatedly washed until the conductivity of the filtrate was approximately 100 μS. Finally, the samples were dried overnight in air at 100 °C.

Subsequently, a 10 g portion of the dry permutite was treated with 12 g of glacial acetic acid (Fisher) and 100 mL of distilled water. The sample was allowed to stir at 70 °C for 15 min and then filtered. The acetic acid treatment was repeated for a second time. The permutite was filtered and washed until the pH of the filtrate was greater than 4. The acid-treated sample was dried overnight in air at 100 °C.

Structural Characterization. Powder X-ray diffraction (XRD) patterns were recorded at room temperature on a Siemens Kristalloflex D 500 diffractometer (Cu Kα radiation, Kevex detector, 40 kV, 30 mA; $2\theta = 5-60°$, 0.05° step size and 3 s count time) and used for crystalline phase identification. The phases were identified by comparison with the data reported in the JCPDS (Joint Committee of Powder Diffraction Standards) database.

Energy dispersive spectroscopy (EDS) and scanning electron microscopy (SEM) were performed for stoichiometric determination of phases, particle size, and morphology. The instrument used was a JEOL JSM-6300V scanning electron microscope with the LINK GEM light-window energy dispersive spectrometer. Samples were deposited on carbon tape and coated with 5 nm of gold to prevent charging. Five random spots in each sample were chosen to collect chemical composition data and the average value of these five measurements was used in the calculations.

Transmission electron microscopy (TEM) was performed on a Philips CM30 TEM operating at 300 kV for bright field and dark field imaging. A Thermo Noran NSS300 EDS spectrometer was used for elemental analysis. The samples were supported on a holey carbon grid.

Differential thermal analysis (DTA) and thermogravimetric analysis (TGA) were performed on a TA Instruments STD 2960 Simultaneous DTA-TGA with alumina crucibles and alumina powder reference. The heating profile consisted of a 5 °C min^{-1} linear ramp from ambient temperature to 600 °C in a static air atmosphere.

Surface analysis was achieved by nitrogen physisorption at −196 °C using a Micromeritics ASAP 2010 instrument. Prior to analysis, the samples were degassed to 0.5 Torr at 200 °C. The surface areas were calculated by the Brunauer−Emmet−Teller (BET) method, assuming a cross-sectional area of 0.162 nm^2 for the N_2 molecule. The pore volume was assessed by the Barrett−Joyner−Halenda (BJH) technique, which is assumed to cover the cumulative adsorption volume of pores with a maximum diameter of 1.7−300 nm.

Fourier transform infrared (FT-IR) spectroscopy was performed on a Perkin-Elmer FTIR Spectrometer GX. The samples were prepared with KBr and pressed into wafers. Spectra were collected in the mid-IR range of 400 to 4000 cm^{-1}, with a resolution of 2 cm^{-1}.

Solid state ^1H, ^{23}Na, and ^{27}Al magic-angle-spinning (MAS) NMR experiments were performed on a Bruker Avance 400 MHz spectrometer with a 4 mm HXY Bruker MAS probe. The ^1H, ^{23}Na, and ^{27}Al NMR measurements were recorded at a spinning rate of 12 kHz, with single pulse-acquire pulse sequences. ^{23}Na and ^{27}Al MAS NMR experiments were performed with an excitation

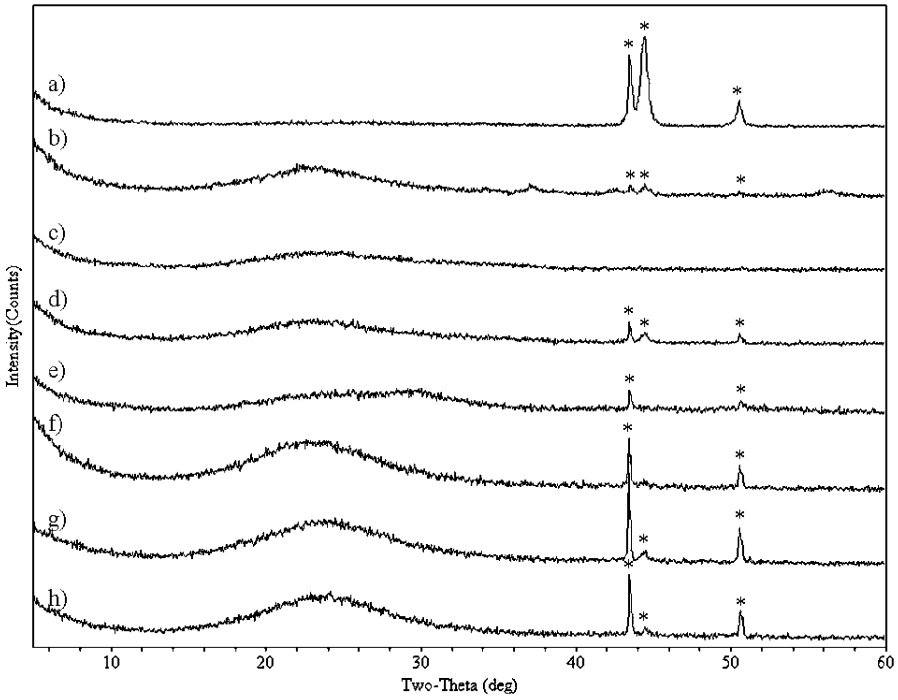

Figure 1. Powder diffraction patterns of select permutite samples: (a) Mn, as-synthesized; (b) Mn, acid-treated; (c) Fe, as-synthesized (note: a glass slide was used to avoid peaks from holder); (d) Fe, acid-treated; (e) Y, as-synthesized; (f) Y, acid-treated; (g) 15% Al, as-synthesized; (h) 15% Al, acid-treated. Peaks marked with (*) are from the sample holder. Diffraction patterns were taken at room temperature in air.

pulse of 0.2 μs (~1/10 of the selective $\pi/2$ pulse length of 2.5 μs) and a recycle delay of 250 ms. The ^{23}Na and ^{27}Al chemical shifts were reported relative to 0.1 M solutions of NaOH and $Al(NO_3)_3$, respectively. The ^{1}H MAS spectra were obtained with $\pi/2$ pulse lengths of 3.5 μs.

^{27}Al MAS data were quantified in two ways. In the first, the ^{27}Al MAS spectra were fit to overlapping semi-Gaussian peaks centered at ~55, 35, and 8 ppm. The relative mole fractions of the four-, five-, and six-coordinate alumina species were calculated using the fractional areas. Absolute quantification of the species was determined by multiplying the relative mole fractions by the total aluminum content from the elemental analysis, wt % AlO_6 = $\%AlO_{6-rel}$ * Al wt %, for each composition.

Solid state ^{29}Si NMR measurements were acquired on a Chemagnetics CMX-300 spectrometer with a 7.5 mm CPMAS probe. The ^{29}Si MAS NMR measurements were recorded at a spinning rate between 2 and 4 kHz, with single pulse-acquire with high power proton decoupling pulse sequences with an excitation pulse of 7 μs and a recycle delay of 300 s. The ^{23}Si chemical shift was reported relative to neat tetramethylsilane (TMS). ^{29}Si cross polarization MAS experiments were performed with similar conditions and 45 kHz spin locking pulse on both channels for Hartmann-Hanh matching for cross polarization. CW decoupling at 60 kHz was applied during acquisition. The recycle delay for the CPMAS experiments was 4 s.

Ionic Exchange Capacity Measurement. The ionic exchange capacity (IEC) for permutite was measured by reacting 1 g of acid-treated permutite with 50 mL of 0.1 M NaOH (aq) for 15 min at 70 °C. Then, the permutite was filtered and washed. The filtrate was collected and titrated with 0.1 M HCl (aq). The IEC, expressed as milliequivalents per gram (mequiv g^{-1}), was calculated using the following equation:

$$\mathrm{IEC} = [(M_{\mathrm{NaOH}} \times V_{\mathrm{NaOH}}) - (M_{\mathrm{HCl}} \times V_{\mathrm{HCl}})]/\mathrm{mass}_{\mathrm{permutite}}$$

The IEC was measured three times per sample to get an average.

Chemical Regeneration. Spent permutite samples, containing 22.8% Al, were chemically regenerated by the acid-treatment procedure described above using either H_2SO_4 (Fisher) or glacial acetic acid (Fisher). The IEC was remeasured to study the number of times that permutite can be regenerated.

Results and Discussion

Synthesis and Structural Characterization. Three different series of permutite were synthesized: (A) The Al mole percent varies between 0 and 25% using sodium silicate with a SiO_2/Na_2O wt ratio of 2.40; (B) the Al content is constant at 22.8 mol % while the SiO_2/Na_2O wt ratio of the sodium silicate varies; and (C) the M^{3+} cation is altered, but the M^{3+} mole percent and the sodium silicate SiO_2/Na_2O wt ratio are constant at 15% and 2.40, respectively. Examination of the powder diffraction patterns (Figure 1) reveals a broad diffraction peak near $2\theta = 30°$, which is characteristic of an amorphous solid. No crystalline phases were detected in the samples with one exception: the acid-treated Mn-permutite displays two unidentified peaks at $2\theta = \sim37.1°$ and ~56.3°. Note, the peaks located at $2\theta = 43.4°$, 44.5°, and 50.6° are due to the sample holder.

Under the experimental conditions it is possible that short-range order exists, which would not be detected by powder XRD. Further examination of the samples by TEM supports that the as-synthesized and acid-treated Al-permutite samples are amorphous on the nanoscale, except for the 25 mol % Al-permutite (Figure 2). The amount of crystalline material detected was minimal. The *d*-spacing could not be determined as a result of the crystalline material being imbedded in the bulk permutite phase. Elemental analysis indicates little difference between the compositions of the crystalline phase and the bulk permutite.

The physical properties of the samples are summarized in Table 1. EDS confirms that the compositions of the various Al-permutite phases studied ($Na_{x+2y}Al_xSi_{1-x}O_{2+y}$) are within

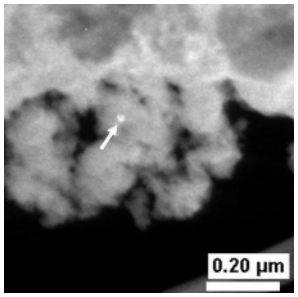

Figure 2. Dark-field TEM micrograph of 25% Al, as-synthesized permutite. The arrow points to the crystallite.

experimental error of the expected values. In all cases the Si/Al ratios of the acetic acid-treated samples remained nearly identical to the pretreated samples, implying that all the Si and Al was retained during treatment. No correlation appears to exist between either the surface area or average pore diameter and the aluminum concentration in the permutite samples or the molecular weight of the M^{3+}. Surface analysis of series B shows that the surface area increases, but the pore diameter decreases with increasing SiO_2/Na_2O ratio of the sodium silicate. Scanning electron micrographs (Figure 3) confirm the small (<100 nm), uniform particle size.

The structural stability of the as-synthesized and acid-treated 15 mol % Al-permutite was investigated by DTA/TGA. Inspection of the DTA data reveals neither endothermic nor exothermic peaks from 25 to 600 °C. The TGA scans show a continuous weight loss of ∼20% for both samples upon heating from room temperature to ∼160 °C. The weight loss is associated with the dehydration of adsorbed water. Furthermore, the powder diffraction patterns of the heated samples indicate that the permutite samples remain amorphous.

In an effort to understand the structural characteristics on the short-range atomic level, FT-IR experiments were performed. Figure 4 shows the FT-IR spectra of select samples; broad bands are due to the distribution of bond lengths and angles as well as the disorder in the relative orientation of the structural units. The vibrational spectra of the as-synthesized and acid-treated samples are similar; no difference can be seen between the Si−ONa and Si−OH species. Bands at ∼455, ∼790, and ∼1165 cm^{-1} are well-described in the literature and correspond to the rocking, bending, and asymmetric stretching modes of the Si−O−Si bridge, respectively.[19−23] The peak at ∼1065 cm^{-1} is attributed to the asymmetric stretching of the Si−O−Si or Si−O−Al tetrahedra of an amorphous aluminosilicate.[20,23,24] The band in the 547−578 cm^{-1} can be associated with structural order, such as rings of tetrahedra and/or octahedra.[25,26] Specifically, this peak is characteristic of the

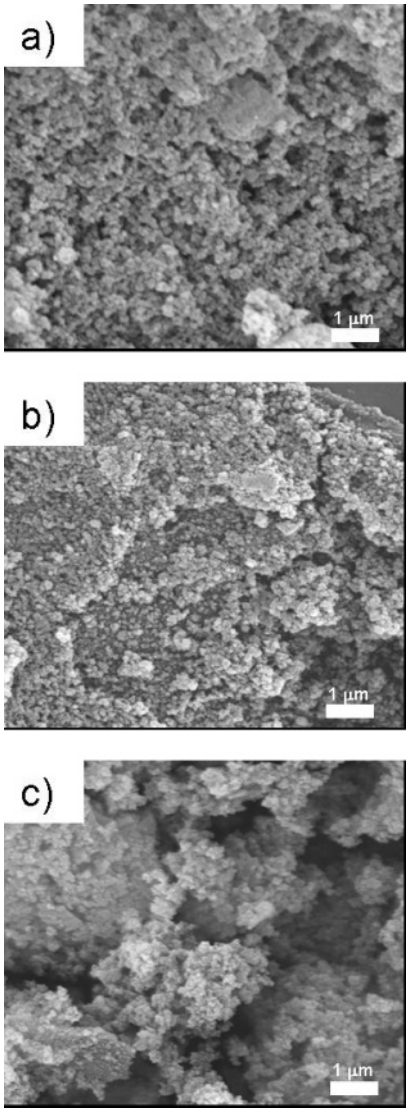

Figure 3. SEM micrographs of select permutite samples: (a) 0% Al, acid-treated; (b) 25% Al, as-synthesized; (c) Y, acid-treated.

stretching frequencies six-coordinate aluminum.[25,27,28] In contrast, the stretching vibrations for AlO_4 are located in the 650−900 cm^{-1} region. The Si−O stretching and OH bending of the Si−OH appear between 898 and 957 cm^{-1}.[19,28] The shoulder at ∼3630 is due to the Si−OH stretching and bridging OH groups.[29] The two remaining peaks at ∼1645 and ∼3460 cm^{-1} are associated with H−O−H bending and −OH stretching of adsorbed water.[19,28] Overlap of the −OH stretching of adsorbed water, SiOH, and bridging OH groups makes the quantification of OH groups difficult. Furthermore, correlations could not be made between the peak position and aluminum concentration.

The IR spectra of the Mn-, Fe-, and Y-permutites match those of the Al-permutite and are similar to published spectra of Mn-, Fe-, and Y-silicates.[30−32] The band assignments given

(19) Farmer, V. C. *The Infrared Spectra of Minerals*; Mineralogical Society: London, 1974.
(20) Gadsden, J. A. *The Infrared Spectra of Minerals and Related Inorganic Compounds*; Butterworth: London, 1975.
(21) Ghosh, S. N. *J. Mater. Sci.* **1978**, *13*, 1877.
(22) Miecnikowski, A.; Hanuza, J. *Zeolites* **1985**, *5*, 188.
(23) Jobic, H.; Smirnov, K. S.; Bougeard, D. *Chem. Phys. Lett.* **2001**, *344*, 147.
(24) Lee, W. K. W.; van Deventer, J. S. J. *Langmuir* **2003**, *19*, 8726.
(25) Poe, B. T.; McMillan, P. F.; Angell, C. A.; Sato, R. K. *Chem. Geol.* **1992**, *96*, 333.
(26) Handke, M.; Mozgawa, W.; Nocuñ, M. *J. Mol. Struct.* **1994**, *325*, 129.
(27) Tarte, P. *Spectrochim. Acta* **1967**, *23A*, 2127.
(28) Farmer, V. C.; Fraser, A. R.; Tait, J. M. *Geochim. Cosmochim. Acta* **1979**, *43*, 1417.
(29) Ratnasamy, P.; Kumer, R. *Catal. Today* **1991**, *9*, 329.
(30) Buciuman, F.; Patca, F.; Craciun, R.; Zahn, D. R. T. *Phys. Chem. Chem. Phys.* **1999**, *1*, 185.

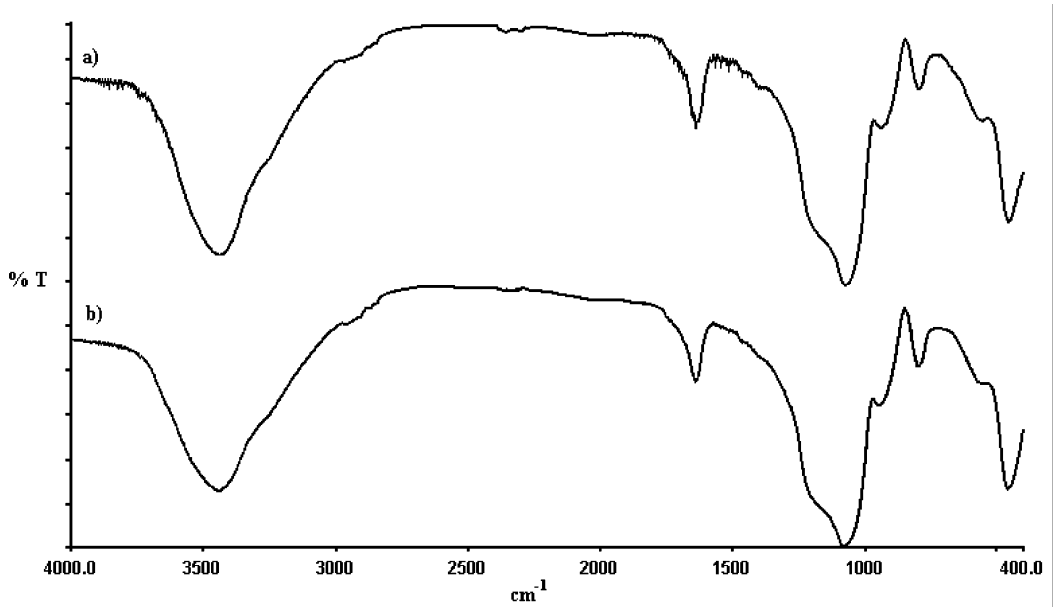

Figure 4. IR spectra of (a) as-synthesized permutite containing 15% Al and (b) acid-treated permutite containing 15% Al.

for the Al-permutite can be extended to the other M^{3+}-permutites synthesized in this study. Negligible differences between the spectra can be explained by the polarization and distortion of SiO_4 tetrahedra surrounding a heteroatom.[32,33] Thus, the change in frequency is determined principally by the polarity and strength of the $M^{\delta+}\cdots O^{\delta-}SiO_3$ bonds. Again, no correlations could be made for peak position and the M^{3+} concentration or between the quantification of OH groups and peak intensity.

Typical solid state ^1H and ^{23}Na NMR spectra of the permutite samples show no difference between the as-synthesized and acid-treated permutite samples. In addition, no variance was observed as the aluminum content increased among the permutite samples. The proton NMR spectrum is dominated by protons associated with water and there is some sign of protons connected with hydroxyls. The position and line shape of the ^{23}Na NMR spectrum are consistent with sodium aluminosilicate glasses, with sodium acting as a network modifier.[34]

The ^{29}Si NMR and ^{29}Si CPMAS spectra obtained (Figure 5) consist of overlapping and not completely resolved broad resonances due to the presence of Q^2, Q^3, and Q^4 species of the amorphous aluminosilicates. $^{29}Si\{^1H\}$ CPMAS experiments were run and show an increase in Q^2 and Q^3 peaks versus MAS NMR. This indicates that some of the proton species are associated with the aluminosilicate framework via Si−OH bonds. No trends were observed in either the MAS or CPMAS spectra with changes in composition. This is not surprising given the complexity of the amorphous structures. In addition to the expected distribution of silicon speciation in the various Q_i sites, one would expect a distribution of the next nearest neighbor speciation (i.e., Si−O−Si, Si−O−Al, and Si−O− Na^+ and Si−OH sites present). The ranges of chemical shifts expected for the composition range studied here would not be, in general, large enough to observe speciation trends with increased Al or Na content.[34]

The ^{27}Al NMR spectra of the as-synthesized and acid-treated permutite are presented in Figure 6. In general, two peaks were observed at ∼55 ppm and ∼5 ppm and are associated with tetrahedrally and octahedrally coordinated aluminum, respectively. In some samples, a non-negligible spectral intensity in the 35 ppm range consistent with five-coordinate AlO_5 sites was also observed. The NMR results obtained here, in general, are in agreement with previous studies on sodium aluminosilicate glasses.[34−37] The resonances are asymmetrically broadened by distributions of chemical shift and first- and second-order quadrupolar couplings due to the disordered amorphous network structure. This broadening makes it difficult to accurately deconvolute the line shapes and as a result quantification was based only on the integral of the spectral intensities from 100 to 20 ppm (tetrahedral, four-coordinate AlO_4) and from 20 to −100 ppm (octahedral, six-coordinate AlO_6). Small systematic errors are expected by this approach due to the presence of small amounts of five-coordinate sites and overlap in the 20 ppm range between the four- and six-coordinate resonances. It is estimated that the total of these systematic errors is less than 5%. For the materials studied here, no significant differences in the chemical shifts are observed between the spectra of the as-synthesized and acid-treated permutite samples; however, the ratio of the areas under the peaks was observed to be a function of surface treatment and composition. The

(31) Scarano, D.; Zecchina, A.; Bordiga, S.; Geobaldo, F.; Spoto, G.; Petrini, G.; Leofanti, G.; Padovan, M.; Tozzola, G. *J. Chem. Soc., Faraday Trans.* **1993**, *89*, 4123.
(32) Saraswati, V.; Raot, S.; Anjaneyulu, K. V. S. R.; Visveswararao, N. V. *J. Mater. Sci.* **1993**, *28*, 1867.
(33) Bordiga, S.; Buzzoni, R.; Geobaldo, F.; Lamberti, C.; Giamello, E.; Zecchina, A.; Leofanti, G.; Petrini, G.; Tozzola, G., Vlaic, G. *J. Catal.* **1996**, *158*, 486.
(34) Eckert, H. *Prog. Nucl. Magn. Reson. Spectrosc.* **1992**, *24*, 159.
(35) Kirkpatric, R. J. S*pectroscopic Methods in Mineralogy and Geology*; Hawthorne, F. C., Ed.; Mineralogical Society of America: Washington, DC, 1988; p 341.
(36) Poe, B. T.; McMillan, P. F.; Angell, C. A.; Sato, R. K. *Chem. Geol.* **1992**, *96*, 333.
(37) Yang, H.; Walton, R. I.; Antonijevic, S.; Wimperis, S.; Hannon, A. *J. Phys. Chem. B* **2004**, *108*, 8208.

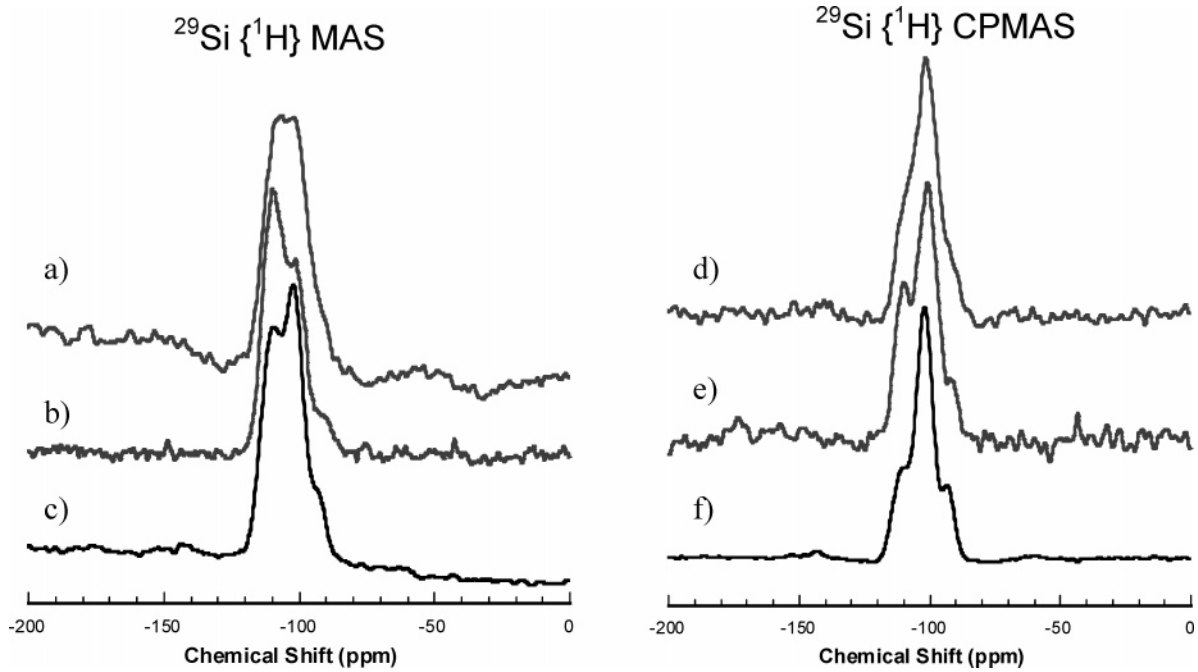

Figure 5. ^{29}Si {^{1}H} MAS NMR spectra of (a) 10% Al, (b) 5% Al, and (c) 0% Al. ^{29}Si {^{1}H} CPMAS NMR spectra of (d) 10% Al, (e) 5% Al, and (f) 0% Al.

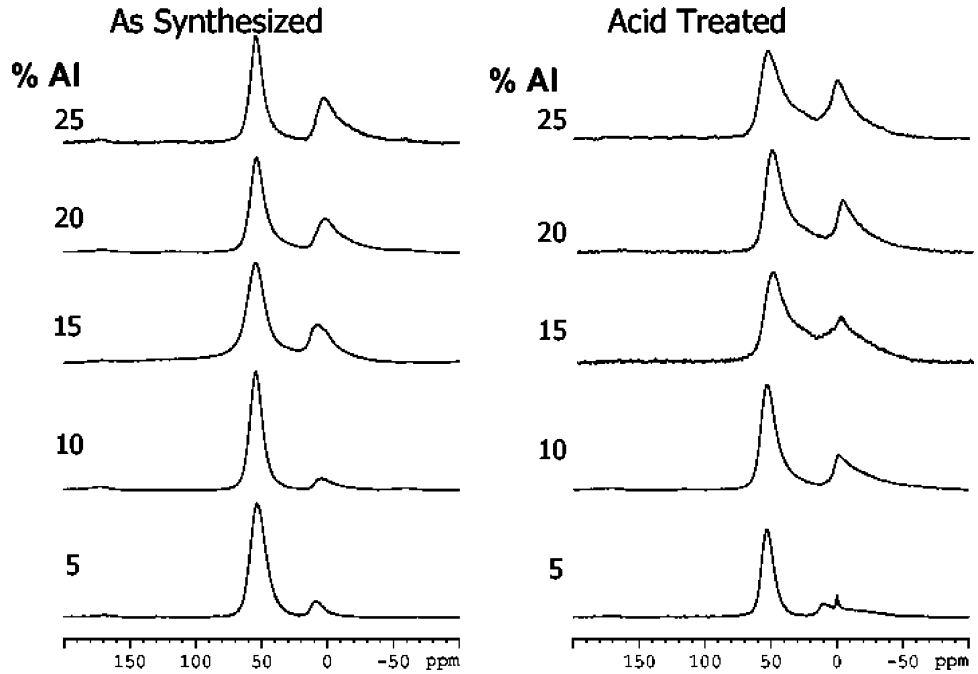

Figure 6. ^{27}Al MAS NMR spectra of permutite samples before and after acid treatment.

observed relative amount of AlO_6 species increased with acid treatment and a general increase in the relative amount of six-coordinate aluminum with increasing aluminum content (Figure 7a) was observed. When converted to absolute speciation, however, the total amounts of both tetrahedral and octahedral species were observed to have increased, as shown in Figure 7b.

A series of ^{27}Al MAS NMR experiments was also performed on samples after ion-exchange measurements. The results of these studies show (Figure 8) that, after exchange, there is a decrease in the amount of AlO_6 species present in all samples. EDS shows a slight decrease in the amount of Al for the ion-exchanged samples. For example, the acid-treated $Na_{0.5+2y}Al_{0.25}Si_{0.75}O_{2+y}$ sample contained 24.6% Al by weight and only 22.3% Al after ion exchange. This suggests that the O_h Al sites are found on the solvent accessible surfaces of the permutite and readily integrated into the framework via transformation to four-coordinate sites. This structural rearrangement has been observed in other systems.[37,38]

Ion-Exchange Capacity Measurements. A summary of the ionic exchange capacity (IEC) values are listed in Table 1. Figure 9 shows the IEC of the Al-permutites increases

(38) Mokaya, R. *Chem. Commun.* **2000**, *19*, 1891. Mokaya, R. *Adv. Mater.* **2000**, *12*, 1681.

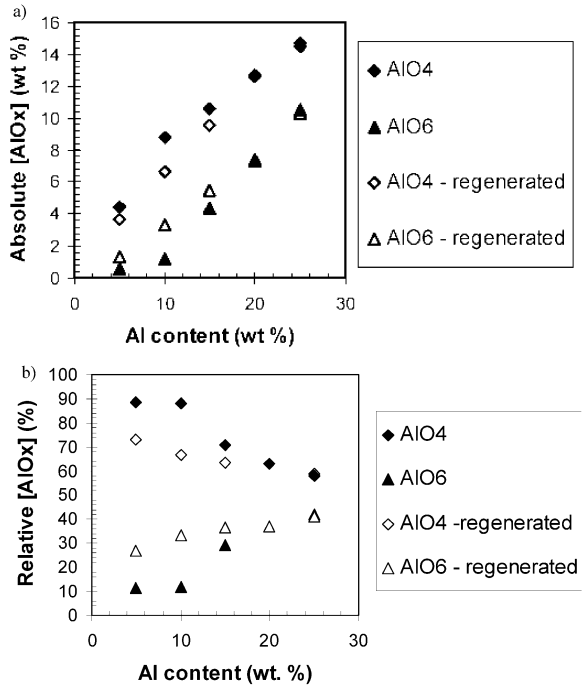

Figure 7. (a) Plot of the relative integrated area under the peaks observed in the ^{27}Al MAS NMR. (b) Plot of the absolute weight % of Al as tetrahedral and octahedral species derived from the ^{27}Al MAS NMR as described in the text.

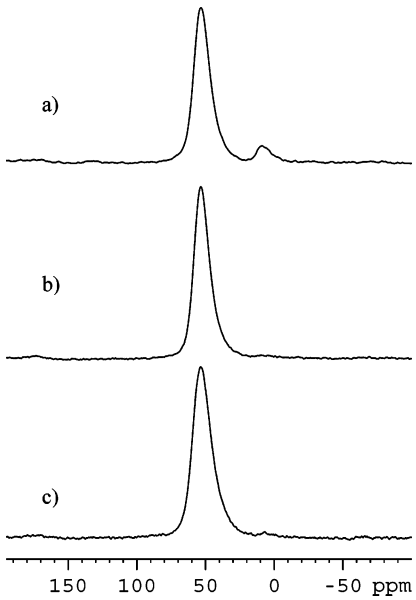

Figure 8. ^{27}Al MAS NMR of ion-exchanged permutite samples: (a) 25% Al, (b) 15% Al, and (c) 5% Al.

with increasing aluminum content (i.e., % Al). Ion exchange in the 0% Al-permutite is only related to the terminal −OH of the silanol groups (Brönsted acid sites). The increased IEC observed with increasing [Al] is due to the addition of new Lewis acid sites (four-coordinate, Si−O$^{(-)}$−Al lattice). This phenomenon has been observed in several aluminosilicates.[38−40] The presence of a crystalline phase might explain the decrease in the IEC of the 25% Al-permutite.

(39) Mozgawa, W.; Fojud, Z.; Handke, M.; Jurga, S. *J. Mol. Struct.* **2002**, *614*, 281.
(40) Houde-Walter, S. N.; Inman, J. M.; Dent, A. J.; Greaves, G. N. *J. Phys. Chem.* **1993**, *97*, 9330.

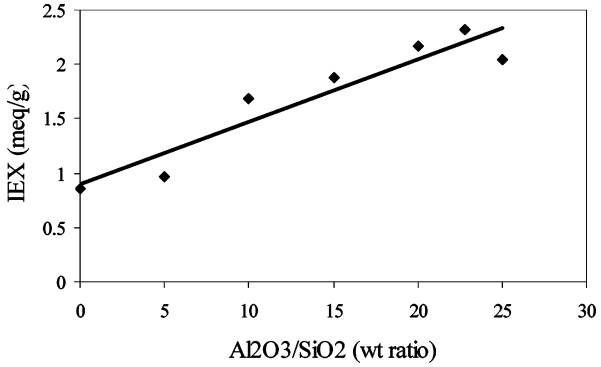

Figure 9. Plot of the ion-exchange capacity versus the aluminum composition in permutite.

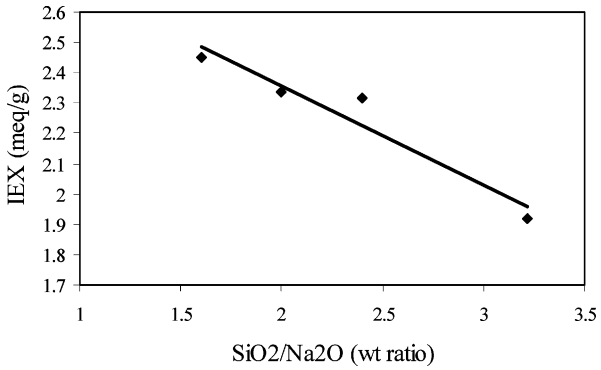

Figure 10. Plot of the ion-exchange capacity versus the SiO_2/Na_2O weight ratio of the sodium silicate reagent.

Additionally, the IEC increases with decreasing SiO_2/Na_2O weight ratio (Figure 10). One circumstantial explanation is that the additional sodium results in enhanced pore accessibility (Table 1) to the ion-exchange sites. However, this causes more salt to be removed during the sample washing than with samples synthesized using lower SiO_2/Na_2O ratios. Our optimized SiO_2/Na_2O weight ratio is 2.00 as a compromise between the amount of washing and IEC of the permutite.

The general formula of permutite is $Na_{x+2y}M^{3+}{}_xSi_{1-x}O_{2+y}$, where M^{3+} = Al, Mn, Fe, Y. In these studies, the maximum IEC have been observed where M^{3+} = Al. To date no correlations can be made between the molecular weight or ionic radii of the M^{3+} atoms and the IEC values. In addition, there is evidence of metal leaching from the Mn and Fe-permutite phases during IEC experiments, as observed by H_2O discoloration. Further studies of the M^{3+} coordination are ongoing.

Finally, the IEC values do not appear to correlate with the BET measured surface area (on dry samples) and pore volumes. This may result from differences in the surface characteristics during each measurement, as the IEC values were measured in aqueous systems and the surface analyses were performed in a dry environment.

Regeneration Studies. Spent 22.8% Al-permutite was regenerated by acetic acid and sulfuric acid. The IEC values are shown in Table 2. The IEC values of the permutite regenerated by acetic acid are within experimental error of the initial value. However, the IEC of the sulfuric acid regenerated samples decreases significantly with additional regenerations and approach the value of the amorphous

Table 2. Regeneration of 22.8% Al-Permutite

regeneration no.[a]	IEC value (mequiv g^{-1})
initial value	2.32
AA-1	2.22
AA-2	2.19
AA-3	2.23
SA-1	1.20
SA-2	1.09
SA-3	1.03

[a] AA = acetic acid. SA = sulfuric acid.

silicate, implying that the aluminum is being leached by the sulfuric acid. This observation is consistent with the use of sulfuric acid for dealuminating zeolites.

This study shows that permutite-like amorphous silicates display a high ion-exchange capacity and the IEC can be easily regenerated. These properties make permutite an attractive material for the patent pending desalination process of brackish waters using ion-exchange materials.[41,42]

We continue to explore the relationship between this class of amorphous materials and their ion selectivity. Ongoing studies include the role of M^{3+} lattice substitution, competitive cation exchange, and durability of the materials.

Conclusions

A series of amorphous silicates with the general formula $Na_{x+2y}M^{3+}{}_xSi_{1-x}O_{2+y}$ (M^{3+} = Al, Mn, Fe, Y) has been prepared to study the cation-exchange capacity. From the data presented above, the ion-exchange capacities of $Na_{0.3+2y}M^{3+}{}_{0.15}Si_{0.85}O_{2+y}$ (M^{3+} = Al, Mn, Fe, Y) decrease as follows Al > Fe > Mn > Y. The ion-exchange capacities of the amorphous aluminosilicate increased with increasing aluminum concentration. This can be explained that ion exchange of the 0% Al-permutite is only related to Brönsted acid sites, but the IEC increases with the formation of Lewis acid sites upon incorporation of aluminum. Furthermore, spent 22.8% Al-permutite can be regenerated with acetic acid and show minimal loss of the initial ion-exchange capacity.

Structural investigations of the as-synthesized and acid-treated Al-permutite samples show that no long-range order exists within the samples. Solid-state NMR experiments show that the relative amount of six-coordinate Al species to four-coordinate Al species increases with increasing aluminum concentration, but there is an increase in the total AlO_4 species. The IEC of permutite is associated with the tetrahedral aluminum sites.

The high ion-exchange capacity and ability to regenerate that is exhibited by the 22.8% Al-permutite sample make permutite an attractive material for the desalination of brackish waters. These results illustrate the importance of determining the local structure of the ion-exchange sites in atomic detail. A fundamental understanding of the structure/property relationship of permutite will allow for the potential development of materials with higher ion-exchange capacities.

Acknowledgment. The authors thank M. Hightower, T. Hinkebein, D. Horschel, J. Krumhansl, A. Sattler, and J. Voigt for helpful discussions. Sandia is a multiprogram laboratory operated by Sandia Corporation, a Lockheed Martin Company, for the U.S. DOE's National Nuclear Security Administration under Contract DE-AC04-94AL85000. Portions of this work were performed under the auspices of the U.S. DOE by the University of California Lawrence Livermore National Laboratory under Contract No. W-7405-ENG-48.

CM050547I

(41) Nenoff, T. M.; Phillips, M. L. F.; Pless, J. D. U.S. Patent, filed 2004.
(42) Pless, J. D.; Krumhansl, J. L.; Voigt, J. A.; Moore, D.; Axness, M.; Phillips, M. L. F.; Sattler, A.; Nenoff, T. M. *Desalination of Brackish Ground Waters and Produced Waters Using In-situ Precipitation*; SAND2004-3908; Sandia National Laboratories: Albuquerque, NM, 2004.